BAYESIAN STRATEGIES FOR SIMULATION-BASED OPTIMISATION AND RESPONSE SURFACE CREATION USING A SINGLE TOOL. APPLICATION TO HYDROFOIL OPTIMISATION

P. Ploé, R. Lanos, Michel Visonneau, J. Wackers

BAYESIAN STRATEGIES FOR SIMULATION-BASED OPTIMISATION AND RESPONSE SURFACE CREATION USING A SINGLE TOOL. APPLICATION TO HYDROFOIL OPTIMISATION.

P. Ploé, Ecole Centrale de Nantes / CNRS / STREAMLINE, France, patrick.ploe@ec-nantes.fr
R. Lanos, STREAMLINE, France, romain@sline-solutions.com
M. Visonneau, Ecole Centrale de Nantes / CNRS, France, michel.visonneau@ec-nantes.fr
J. Wackers, Ecole Centrale de Nantes / CNRS, France, jeroen.wackers@ec-nantes.fr

Surrogate models are simplified models for the behaviour of a complex system, based on a limited number of operating points where the system behaviour is simulated accurately. In hydrofoil design for sailing yachts, surrogate models can be used both for automatic shape optimisation of the foil and for performance evaluation of the entire yacht in the context of a VPP, as a response surface. We present an adaptive method for the construction of surrogate models which can be used for both these objectives, with a simple change of parameters. A Gaussian process regression (GPR) is used for the data fitting, while the adaptive choice of sample points is based either on the GPR variance or on a combination with a cross-validation error estimation. A first test on analytical functions shows that the cross-validation approach is superior for response surface creation, while both adaptation methods are equally suited for shape optimisation. A second test on the shape optimisation of a two-dimensional hydrofoil indicates that for moderate immersion depths, the optimum shape is not sensible to the distance to the free surface.

1 INTRODUCTION

Most engineering design processes rely on physical or numerical experiments to evaluate the candidate design performances. When the design space is large, when the model response is complex, or especially when performing global optimization, many evaluations are required. However, the number of simulations is usually limited by time or financial cost. Hydrofoil optimisation for naval applications is typically facing these limitations.

On way to address this limitation is to build a simplified model of the actual model from responses of experiments. Meta-modelling is the process of generating such models of models or meta-models. This process is also referred in engineering as *surrogate modelling*. Strategies involving surrogate models are recognized in a wide range of engineering fields to efficiently address computational cost limitations. Evaluations of a surrogate model are cheap and can be used for visualization, trade-off analysis and optimization.

Building a surrogate requires evaluating the original model at specified points and gathering the corresponding responses. The amount of sample points needed to approximate the behaviour of a numerical model depends on the complexity of the response, which is not necessarily known beforehand. The chosen sampling strategy plays an important role in the performance of the surrogate model: under-sampling might not allow capturing the complexity of the phenomena and over-sampling could lead to prohibitive computation times. Adaptive sampling or response-adaptive design uses the responses to the experiments for adjusting the sampling in a sequential way while the surrogate is being constructed. This allows for determining and minimizing the required number of experiments for efficient global surrogate construction.

Hydrofoil optimisation can be performed in different ways. Hydrofoils can be either optimized independently from the rest of the ship they will be fitted to or, in a more robust way, by taking into account the whole ship and simulating its behaviour in a third party simulating code (VPP for instance). We usually switch from one approach to another according to the design stage. Surrogate models can be used for both approaches but, if built in adaptive way, will be sampled quite differently. If the goal is response surface creation for the use in a VPP, exploration (sampling from areas of high uncertainty) will be favoured, in order to create a response surface which is reliable everywhere. Automatic geometry optimisation on the other hand requires exploitation (sampling from areas likely to offer improvement over the current best observation) which means that the sampling area is concentrated close to the optimum.

In this study we investigate the possibility of both creating response surfaces and perform shape optimisation with the same tool. We chose Gaussian process regression (GPR), also known as kriging, to create the surrogates (section 2). After defining an initial set of points using a traditional design of experiment method, the following points are chosen in a sequential and adaptive way. An appropriate acquisition function (also known as infill sampling criterion) has been investigated to access the exploration/exploitation trade-off. The

adaptive sampling is described in section 3. The efficiency of the adaptive sampling is tested on analytical functions (Three hump camel and Gramacy-Lee) in section 4, both for optimisation and for response surface creation. Finally, in section 5 the procedure is applied to the optimisation of a 2D hydrofoil NACA profile. The profile is optimised both in deep water and close to the free surface, in order to assess whether the optimum shape depends on the proximity of the surface.

2 SURROGATE MODELLING

This section first introduces surrogate models in a general setting, then describes the Gaussian process regression employed in the current paper.

2.1 DEFINITION OF SURROGATE MODELS

Let a function $f\colon \mathbb{R}^d \to \mathbb{R}$ be defined on a domain $X \subseteq \mathbb{R}^d$. In the context of this paper, f represents the full model and must be considered as expensive to compute. The number of input parameters is d, these can contain either geometry parameters (for shape optimisation) or operational conditions such as velocity and incidence (for response surfaces).

Surrogate modelling aims at generating an approximation to f from points where f is known exactly. Thus, consider a dataset $\mathcal{D}_n$ of n observations, $\mathcal{D}_n = \{(\mathbf{x}_i, y_i)\}_{i=1}^n$, where $\mathbf{x}_i$ is an input vector of dimension d and $y_i = f(\mathbf{x}_i)$ is an evaluation of the function f. Then, for a surrogate-creating algorithm $\mathcal{A}$:

$$\hat{f}(\mathbf{x}; \mathcal{D}_n) = \mathcal{A}(\mathcal{D}_n), \tag{1}$$

the function returned by algorithm $\mathcal{A}$ on a training set $\mathcal{D}_n$, evaluated in the arbitrary point $\mathbf{x}$, is the surrogate model.

The challenge of surrogate modelling is to generate a surrogate that is as accurate as possible, using as few simulation evaluations as possible. A central question is the choice of the sampling points in $\mathcal{D}_n$. As noted in the Introduction, when the goal of the surrogate model is to provide inputs for a VPP, the points must be placed such that $\hat{f}(\mathbf{x}) \approx f(\mathbf{x}),\ \forall(\mathbf{x}) \in X$. However, if the objective is to perform geometric optimisation, i.e. finding:

$$\mathbf{x}^{\text{opt}} = \arg\min_{\mathbf{x} \in X} f(\mathbf{x}), \tag{2}$$

then it may be useful to concentrate the points around $\mathbf{x}^{\text{opt}}$.

The choice of a model $\mathcal{A}$, mathematical or statistical, used for fitting the learning data is the second major question. The ideal model would allow capturing irregularities in the data set and generalise well to different types of functions f. There are many types of surrogate models available, we choose to use the Gaussian process regression (GPR) described in the remainder of this section. Section 3 is dedicated to the sample selection.

2.2 GAUSSIAN PROCESS REGRESSION

Gaussian process regression is a class of methods for interpolation between known data points. It has been widely used since the 1950's in the field of geostatistics where it is known as kriging. Gaussian processes were then extended to more general multivariate input regression problems. The idea of global optimisation based on Gaussian processes dates back to the 1970's [6]. Since the 1990's, increasing work with kernel methods and Bayesian inference applied to machine learning has been widening the use of Gaussian process regression.

A Gaussian process (GP) supposes that the value of a function $f(\mathbf{x}$ in each point $\mathbf{x}$ is a realisation of a stochastic process with a Gaussian distribution. Given a set of known points $\mathcal{D}_n$, it is possible to establish the most likely outcome for the stochastic variable in each point $\mathbf{x}$, i.e. the mean of the variable. This value is used as the surrogate $\hat{f}(\mathbf{x})$.

To establish the relation between two points [7], the *covariance* function, $k(\mathbf{x}, \mathbf{x}')$, also called kernel, is used. The covariance expresses the similarity between two observations (assuming that points lying close together should have similar function values). In the absence of precise knowledge about the function f, a standard form for $k(\mathbf{x}, \mathbf{x}')$ is assumed (see below).

To establish $\hat{f}(\mathbf{x}; \mathcal{D}_n)$, a covariance matrix is computed:

$$K = \begin{bmatrix} k(\mathbf{x}_1, \mathbf{x}_1) & \cdots & k(\mathbf{x}_1, \mathbf{x}_n) \\ \vdots & \ddots & \vdots \\ k(\mathbf{x}_n, \mathbf{x}_1) & \cdots & k(\mathbf{x}_n, \mathbf{x}_n) \end{bmatrix}, \tag{3}$$

as well as a covariance and autocorrelation for the point $\mathbf{x}$:

$$K_* = \begin{bmatrix} k(\mathbf{x}_1, \mathbf{x}) \\ \vdots \\ k(\mathbf{x}_n, \mathbf{x}) \end{bmatrix}, \quad K_{**} = k(\mathbf{x}, \mathbf{x}). \tag{4}$$

The mean and standard deviation in $\mathbf{x}$ then become [7]:

$$\hat{f}(\mathbf{x}; \mathcal{D}_n) = K_*^T K^{-1} \mathbf{Y}_n, \quad \sigma^2(\mathbf{x}) = K_{**} - K_*^T K^{-1} K_*, \tag{5}$$

where $\mathbf{Y}_n$ is the vector containing all the y_i in $\mathcal{D}_n$. The mean is used as the surrogate model value, while the standard deviation gives information on the uncertainty of this value.

2.3 COVARIANCE FUNCTION

The choice of the covariance function is crucial and the ability of the GP to express a rich distribution on functions depends on it. Among the popular choices of kernel, is the squared exponential kernel:

$$k(\mathbf{x}, \mathbf{x}') = \sigma^2 \exp(-\frac{\|\mathbf{x} - \mathbf{x}'\|^2}{2\ell^2}),$$

with hyperparameters $\theta = \{\sigma, \ell\}$; both of which have a default value of 1.

The squared exponential kernel is very smooth and other class of kernels may be needed to fit complex functions. We choose the Matérn kernel as it is more flexible [5]. The Matérn kernel is defined by the general form of:

$$k(\mathbf{x}, \mathbf{x}') = \frac{1}{2^{\nu-1}\Gamma(\nu)} \left(\frac{2\sqrt{\nu}\|\mathbf{x} - \mathbf{x}'\|}{\theta} \right)^{\nu} H_\nu \left(\frac{2\sqrt{\nu}\|\mathbf{x} - \mathbf{x}'\|}{\theta} \right),$$

This kernel is parameterized by the hyperparameters ν and θ.

3 ADAPTIVE SAMPLING

Adaptive sampling (or sequential sampling) consists in selecting the sampling sites during the series of simulations. Each time a sample is evaluated, a new response surface is generated and the next sample is chosen based on this response surface. The process goes on iteratively until a quality or convergence criterion is satisfied. On the contrary, for a non-adaptive experiment all decisions regarding the sampling design have to be made before running the simulations. Thus, with an optimal choice of adaptive sampling criteria, the use of a sequential strategy can allow for a significant reduction of the sample size and consequently lower computational cost.

The algorithm we have chosen uses a two stage approach. To determine an initial response surface, a series of sample sites is selected in advance, using an existing design of experiments approach with a very coarse sampling (we use full factorial with two points in each direction, but other methods like Latin hypercube could also be used). Then, this initial response surface is adaptively refined by adding one sample at the time. The choice of these points is based on an acquisition function, which is described in the remainder of this section.

3.1 Acquisition functions for response surfaces and optimisation

Given a set of observations $\mathcal{D}_n$, if we want to add a new point $\mathbf{x}_{n+1}$ to $\mathcal{D}_n$ in order to enhance the accuracy of the model, how do we select the next query point $\mathbf{x}_{n+1}$? The bayesian approach consists in designing an acquisition function $a(\mathbf{x})$. The acquisition function is an inexpensive function that can be easily evaluated throughout the design space; the next sampling point is selected as the maximum of a:

$$\mathbf{x}_{n+1} = \max_{\mathbf{x}\in X} a(\mathbf{x}). \tag{6}$$

Thus, the optimal distribution of points in $\mathcal{D}_n$ is obtained by choosing a correctly. In general, two sampling strategies can be identified: exploration which is the sampling of points $\mathbf{x}$ where $\hat{f}(\mathbf{x})$ has a high uncertainty (typically, this means areas with few existing points), and exploitation which is sampling around regions of interest in $\hat{f}$ (typically, its minimum).

We introduce a universal formulation for a that is able to perform both exploration and exploitation. This formulation requires that an estimator $U(\mathbf{x};\mathcal{D}_n)$ for the uncertainty in $\hat{f}(\mathbf{x};\mathcal{D}_n)$ is available, and that the region of interest for exploitation is the minimum of f as in equation (2). Then, the acquisition function is given by:

$$a(\mathbf{x};\mathcal{D}_n) = U(\mathbf{x};\mathcal{D}_n) - \beta\hat{f}(\mathbf{x};\mathcal{D}_n), \tag{7}$$

where $\beta \geq 0$ is a trade-off parameter to balance exploration and exploitation. If the surrogate model is to be used as a response surface in a VPP then exploration is always to be preferred, so β is set to zero. For shape optimisation on the other hand, a fixed non-zero value is chosen for β. Thus, in the beginning of the optimisation when few sampling points are available, the uncertainty U is high so a will be dominated by U, favouring exploration. Later on, when more points are added and the overall shape of f is better known, U will diminish and a is dominated by $\hat{f}$. As a result, the acquisition function automatically switches to exploitation.

One of the difficulties in using this criterion lies in the choice of the value assigned to the parameter β. A possible solution is to try a definite number of values for β and test the corresponding infill points.

3.2 UNCERTAINTY EVALUATION

The accurate evaluation of the uncertainty U in $\hat{f}$ is essential for the acquisition function (7). Here, two choices are described: the statistical uncertainty of the GPR and a new, combined estimator.

3.2.1 GPR Variance

The Gaussian process regression method provides at any point the statistical prediction error, or variance $\sigma(\mathbf{x})$ (equation 5). This variable can be used to estimate the uncertainty. However, the GPR variance in a point $\mathbf{x}$ depends mostly on the distance to other points; the actual shape of the function f does not have a major influence on $\sigma(\mathbf{x})$. Thus, when used in a pure exploration setting ($\beta = 0$), this choice will lead to an equidistribution of the points in space, similar to a full factorial sampling. In an optimisation context, the acquisition function (7) with $U = \sigma$ is known as the Lower Confidence Bound approach (LCB) [2, 3].

3.2.2 Custom Error Estimator

As an alternative to the variance, we would like to take into account an actual error estimation for $\hat{f}$ in the acquisition function. One way to estimate this error is to perform cross validation. Leave one out cross-validation (LOO-CV) computes the real model errors in the points $\mathbf{x}_i$ of $\mathcal{D}_n$, by comparing $f(\mathbf{x}_i)$ with the prediction of a GPR based on all the points in $\mathcal{D}_n$ except i itself:

$$e_i = y_i - \hat{f}(\mathbf{x}_i;\mathcal{D}_{n\setminus i}), \tag{8}$$

For the dataset $\mathcal{E}_n = \{(\mathbf{x}_i, e_i)\}_{i=1}^n$, we then construct a surrogate error model:

$$\hat{e}(\mathbf{x};\mathcal{E}_n) = \mathcal{A}(\mathcal{E}_n). \tag{9}$$

To concentrate the sampled points in the regions where the error in $\hat{f}$ is high, the variance is weighted with this error model:

$$U(\mathbf{x};\mathcal{D}_n) = \sigma(\mathbf{x})\left[\alpha\hat{e}(\mathbf{x};\mathcal{E}_n) + (1-\alpha)\right]. \tag{10}$$

The higher the parameter α is chosen, the larger will be the influence of $\hat{e}$. Our reason for not choosing $\alpha = 1$ is that the error model (9) is not perfect, especially for few sample points: the actual error may be high in zones with no sample points and the model cannot see this. Therefore, it is always necessary to sample large regions without any points, which is obtained by including the term $\sigma(\mathbf{x})(1-\alpha)$ in the uncertainty estimator.

4 ANALYTIC BENCHMARK

The performances of the adaptive sampling are tested on two analytic functions (figure 1), Three hump camel and Gramacy-Lee [4]. These are classic benchmark functions for optimisation performance evaluation. We specifically choose these functions to perform evaluation on a relatively smooth function (Three hump camel) and a more complex function (Gramacy-Lee).

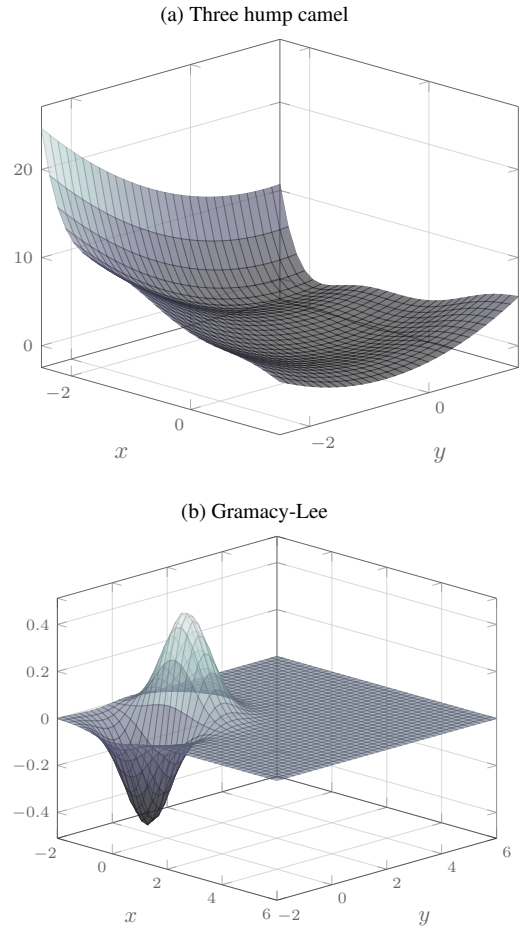

Figure 1: Test functions

4.1 META-MODEL CREATION

The first test evaluates the capabilities of the tool to create a response surface such as would be used in a VPP. The custom acquisition function from section 3.2.2 and the variance-based function from section 3.2.1 are compared with non-adaptive sampling using a full factorial sampling plan. The parameter $\alpha = 0.6$ is used for the custom acquisition function.

Figure 2 shows the evolution of maximum absolute error and mean absolute error as a function of the number of sampled points. For the full factorial approach, only a few values are possible for the number of points (corresponding to 2×2 points, 3×3 points, etc.) Between these points, the shown error values are kept constant.

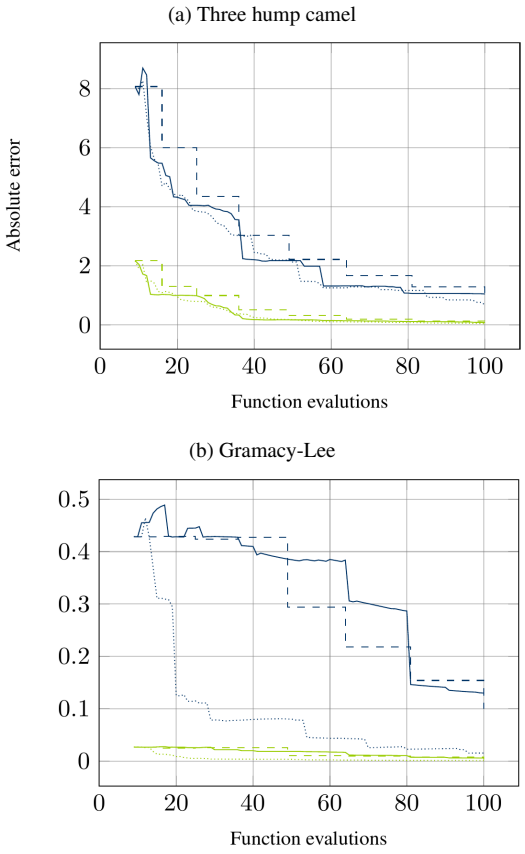

Figure 2: Convergence of absolute error. Blue: maximum error, green: mean error. Drawn lines: variance-based sampling, dots: custom sampling, dashed lines: full factorial.

The figures confirm that the variance-based adaptive sampling has a behaviour which is similar to a full factorial approach, since the global convergence speeds are similar, both for the mean and the maximum errors. However, since the adaptive criterion chooses the current best point to sample at any given moment, its errors can be slightly lower than for the full factorial approach. This is the case for the Three hump camel. In any way, the adaptive approach represents the most intelligent order to compute a full factorial-type sampling plan, since it already produces useful response surfaces for very low numbers of points, which can be used straightaway. Further computations can then be performed to improve the sampling plane.

The performance of the custom acquisition function depends on the problem being solved. For the Three hump camel, its convergence is equivalent to the variance-based sampling, which indicate that this smooth function requires a more or less uniform distribution of sample points for maximum accuracy. Gramacy-Lee on the other hand has its non-zero values concentrated in one part of the domain. The custom sampling is able to detect this and thus perform much better than the other approaches. This is confirmed in figure 7 which shows a plot of the sampled points for the three approaches. The concentration of points created by the custom approach is clearly visible.

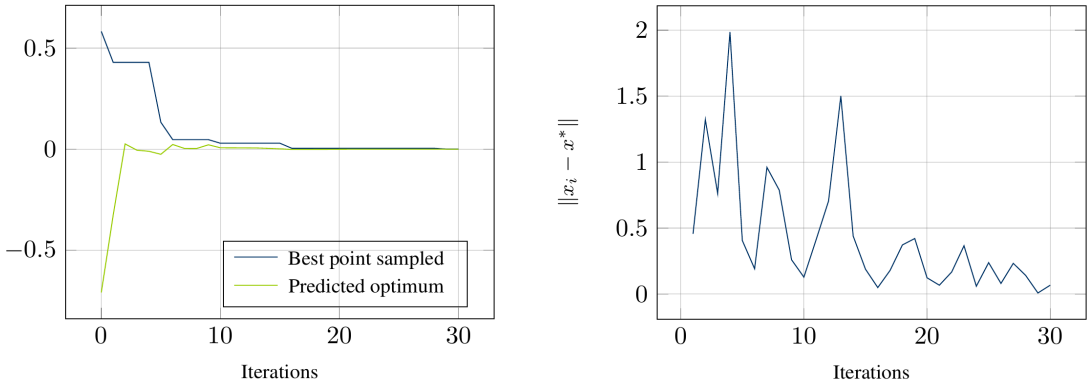

Figure 3: Three Hump Camel, acquisition function: LCB. Left: best observation / prediction. Right: distance to true optimum.

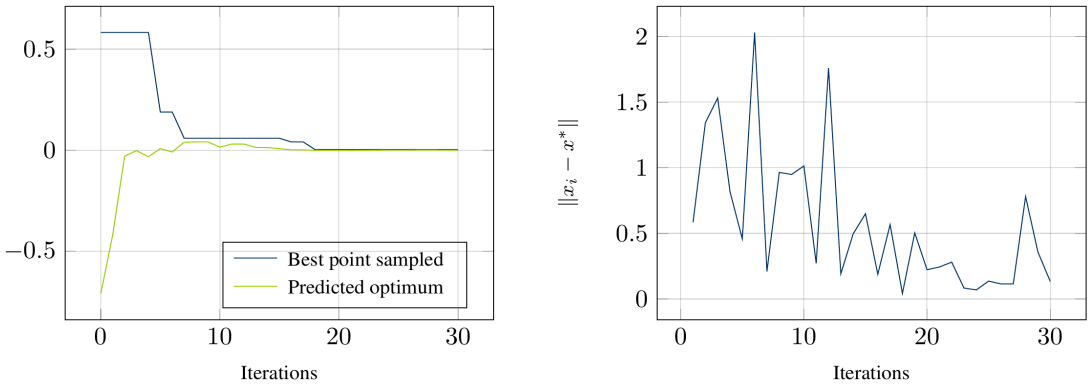

Figure 4: Three Hump Camel, acquisition function: Custom

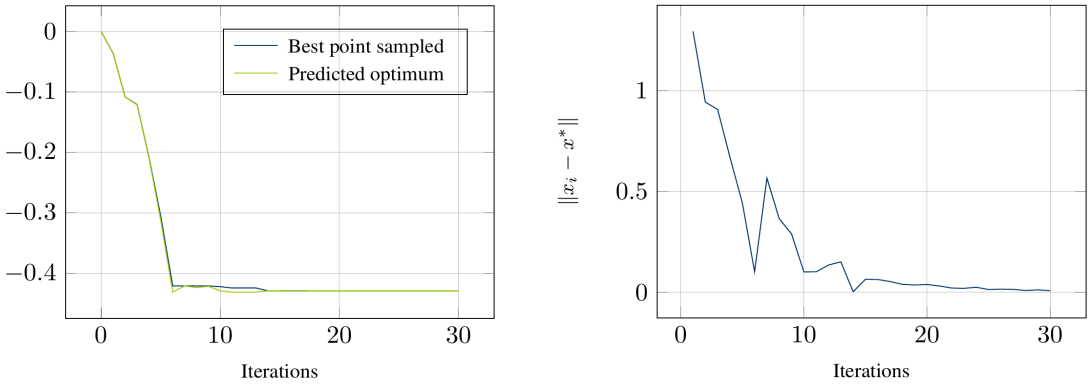

Figure 5: Gramacy-Lee, acquisition function: LCB

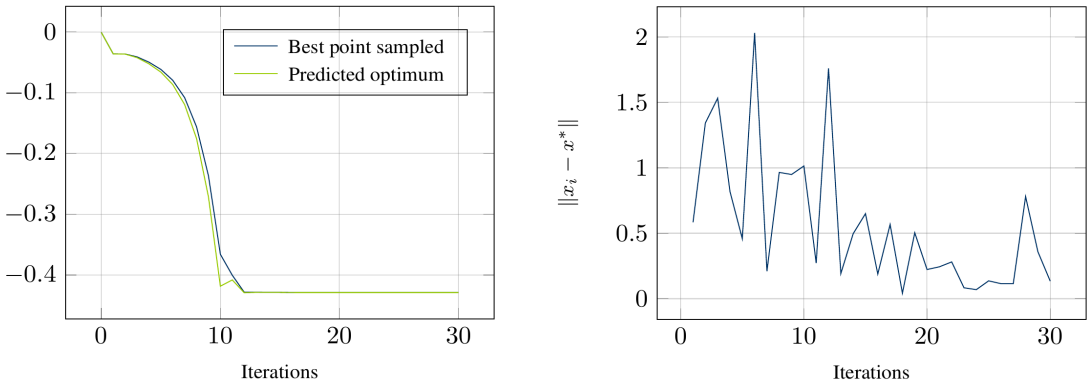

Figure 6: Gramacy-Lee, acquisition function: Custom

(a) Variance-based sampling

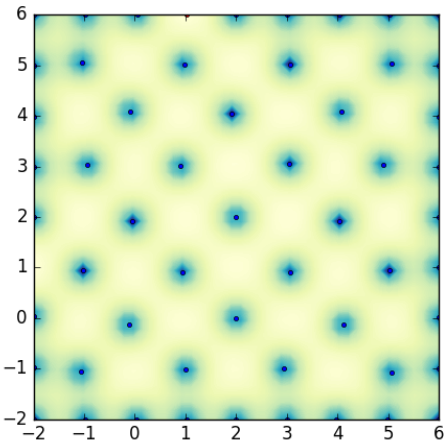

(b) Custom sampling

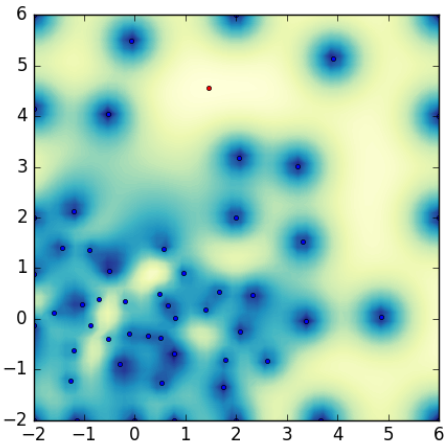

Figure 7: Distribution of sampling points for Gramacy-Lee (55 points). The colouring shows the acquisition function, the lightest colour represents the highest value.

4.2 OPTIMISATION

The custom and variance-based (LCB) criterion are used in an optimisation setting to find the minimum value of the two test functions. As before, $\alpha = 0.6$ is used with the custom function; $\beta = 0.7$ for all cases.

Figures 3 to 6 show the results. To the left in these figures is the minimum value found, both the value in the best point sampled and the minimum value of $\hat{f}$ over the entire domain. It is seen that the latter values converge faster, which means that it is useful to consider the optimum of $\hat{f}$ rather than the best y_i observed.

To the right is the distance from each sampled point to the location of the true optimum. These figures give an impression of the choice between exploration and exploitation, since large distances and oscillatory behaviour indicate exploration, while successive values close to the optimum are typical for exploitation. In all cases, exploration in the beginning gives way to exploitation, although a certain exploratory character remains. However, in the end the exploration is concentrated close to the optimum.

Finally, for optimisation problems it is found that the custom acquisition function loses its clear advantage over the variance-based function for Gramacy-Lee. In fact, the goal of the custom function is to concentrate points in those regions where f varies most, in order to gain efficiency. However, in an optimisation setting the points are placed close to the optimum so they are also being clustered with LCB. Initially, LCB converges even faster than the custom function, although the final step towards the optimum requires an equal amount of iterations.

5 2D PROFILE OPTIMISATION BASED ON RANS SIMULATIONS

The objective of the second test case is to use the method described above to optimise a two-dimensional hydrofoil profile. The optimisation is performed in two conditions: monofluid, and below a free surface. The goal of this test is to determine if the presence of the free surface has an inflence on the optimum geometry.

5.1 SETTINGS

To simplify the geometry generation, the profiles are based on the NACA four-digit series [1] which has three geometry parameters, of which we optimise two: the thickness and maximum camber (figure 8). The ranges allowed for these parameters are $[0.03, 0.15]$ for the thickness and $[-0.02, 0.10]$ for the camber. The x-position of maximum camber is set at 0.4. The velocity is $V = 10m/s$, chord $c = 1m$, density $\rho = 1026kg/m^3$, and Reynolds number $Re = 8.41 \cdot 10^6$. For the free-surface simulations, the trailing edge is placed at $1m$ below the undisturbed water level.

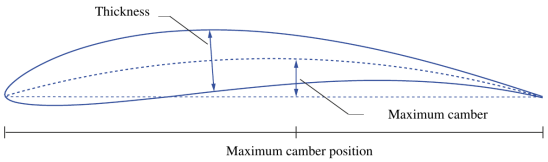

Figure 8: NACA 4-series geometry parameters

The objective for the optimisation is the minimisation of the drag; to obtain a fair comparison of the different geometries, all simulations are performed at the same lift coefficient $C_l = 0.6$. The angle of attack is adjusted dynamically during the simulations in order to obtain this constant lift coefficient. The constants for the acquisition function are $\beta = 0.014$ and $\alpha = 0.012$.

RANS simulations are performed using the FINE^{TM}/Marine computing suite, which includes the finite-volume flow solver ISIS-CFD developed by our group.

For the free-surface simulations, the surface is captured using adaptive grid refinement.

5.2 RESULTS

The results of the two optimisations, the geometry parameters and force coefficients, are provided in table 1. Figure 9 gives the two optimised geometries at their operational angle of attack, while figure 10 shows the pressure coefficient on the two profiles. Finally, the free-surface deformation for the free-surface optimised profile is provided in figure 11.

Table 1: Optimised profile parameters and drag coefficient. The cross-validated C_d is the drag when the optimum monofluid profile is put in free-surface conditions and vice versa.

Case	Thickness	Camber	C_d	C_d cr.-v.
Monofluid	0.0300	0.0449	0.0160	0.0250
Free surface	0.0300	0.0487	0.0249	0.0161

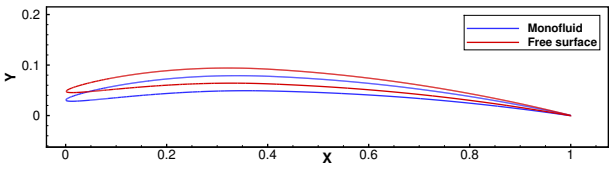

Figure 9: Geometries of optimised profiles

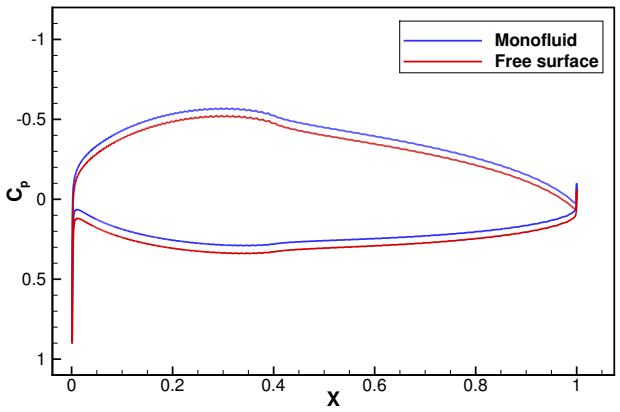

Figure 10: Distribution of the pressure coefficient C_p on both optimised profiles

These figures show that both optimal geometries are very similar. The main difference between the cases is that the presence of the free surface reduces lift, which means that the airfoil has to work at a higher angle of attack to obtain $C_l = 0.6$ (2.74°, while monofluid needs 1.75°). This explains the higher drag for the free-surface condition. The optimal shapes are very thin, almost sail-like profiles, whose leading edges are aligned with the incoming flow. This is shown by the pressure distribution, which has no discernible suction peak on the leading edge. Since NACA four-digit profiles are known for very sharp leading-edge suction peaks, this proves that the camberline is aligned with the incoming flow.

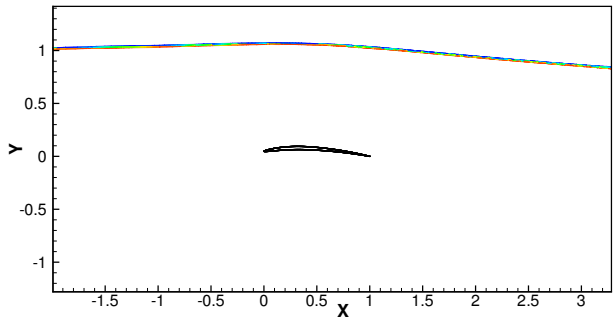

Figure 11: Free-surface position for free-surface optimised profile

5.3 ROBUSTNESS OF THE OPTIMUM

This optimisation exercice has shown that, at least for moderate immersion depths, the shape of the optimum profile is not sensitive to the immersion depth. The optimum shape parameters for the two cases are close, while each shape performs almost as good as the other when placed in the other's situation (table 1). This is good news, since it means that hydrofoils can operate efficiently at different immersion depths. Further studies using more advanced profile shapes and larger numbers of geometrical parameters have to confirm these initial findings.

However, while the dependence of the optimum on the lift coefficient was not tested, it is clear that the very thin profiles obtained are optimised for one angle of attack. Small changes in incidence would lead to separation at the leading edge and a significant increase in drag. Furthermore, the shapes obtained are impractical from a construction point of view.

Thus, hydrofoil optimisation for practical application requires either geometrical constraints or multi-point optimisation. Both can be performed with our technique. For example, a minimum thickness can be specified easily by limiting the range of the design parameters, while the objective function could be changed from the drag at one lift coefficient to a weighted average of the drag at two or more operating points. We plan to study these approaches in the near future.

6 CONCLUSION

This article presented a method for sequential, adaptive sampling in the construction of Gaussian process surrogate models, which can be used both for the construction of response surfaces and for automatic shape optimisation. Two acquisition functions were studied: a classical criterion based on the variance of the GPR model and a new criterion based on Leave-One-Out cross validation errors. The examples have highlighted the efficiency of the suggested criterion: for functions with local peaks, it provides results significantly better than classical criteria and for other functions its performance is equivalent to them.

An optimisation exercice using RANS simulation showed that the method can be used for the shape optimisation of hydrofoils. The optimum shape is found to be insensitive to the presence or absence of a free surface. However, the exercice also showed that thin profiles are produced, which are sensitive to incidence changes. Multipoint evaluation or constrained optimisation can resolve this problem; both will be considered for further study.

REFERENCES

[1] Ira H Abbott and Albert E von Doenhoff. *Theory of Wing Sections, Including a Summary of Airfoil Data*. Dover, 1959.

[2] Dennis D Cox and Susan John. A statistical method for global optimization. In *Systems, Man and Cybernetics, 1992., IEEE International Conference on*, pages 1241–1246. IEEE, 1992.

[3] Dennis D Cox and Susan John. SDO: A statistical method for global optimization. In *in Multidisciplinary Design Optimization: State-of-the-Art*, pages 315–329, 1997.

[4] Robert B Gramacy and Herbert KH Lee. Gaussian processes and limiting linear models. *Computational Statistics & Data Analysis*, 53(1):123–136, 2008.

[5] Bertil Matérn. *Spatial variation*. PhD thesis, Stockholm University, 1960.

[6] J Močkus. *On bayesian methods for seeking the extremum*, pages 400–404. Springer Berlin Heidelberg, Berlin, Heidelberg, 1975.

[7] CE Rasmussen and CKI Williams. *Gaussian Processes for Machine Learning*. Adaptive Computation and Machine Learning. MIT Press, Cambridge, MA, USA, January 2006.

7 AUTHORS BIOGRAPHY

P. Ploé is a naval architect and material engineer. He worked in composite yacht building before joining STREAMLINE in 2013 and starting a PhD on hydrofoil shape optimization. His PhD project is performed in collaboration with the LHEEA Lab, ECN/CNRS.

R. Lanos is a naval architect and engineer. He has created STREAMLINE in 2011 and specialized its activity into the performance prediction and optimization for sailing yachts, developing and using VPPs, CFD tools and working appendages conception and optimization. He has been working on major yacht racing projects, as a member of Groupama Sailing Teams from 2009 to 2016 (Groupama 4 Volvo Open 70, Groupama C C-Class, Groupama 50 AC Class) and more recently on Sodebo 5 Ultim Multihull. He is also professor at the Ecole Nationale Supérieure dArchitecture de Nantes, teaching performance prediction (VPP) and CFD in the frame of the naval architecture diploma (DPEA Architecture Navale).

M. Visonneau obtained in 1980 an Engineer's diploma and the diploma of Advanced Naval Architecture in 1981 from Centrale Nantes. In 1985, he got a PhD of Fluid Dynamics and Heat Transfer of the University of Nantes and entered the National Center for Scientific Research (CNRS) as research associate. He was the head of the CFD department of the Fluid Mechanics Laboratory (Centrale Nantes) from 1995 to 2012. In 2001, he defended his Habilitation to supervise Research and was promoted research director at CNRS in 2006. He has supervised more than 20 PhD thesis. He is a member of the Steering Committee of the International Workshop on CFD in Ship Hydrodynamics since 2005. He was awarded the 2nd Cray prize for CFD in 1991 and 30th Georg Weinblum lecturer in 2007. In 2006, he built a partnership with NUMECA Int. which gave birth to FINE/Marine and is now in charge of the scientific management of this worldwide distributed software.

J. Wackers is a researcher at LHEEA Lab, ECN/CNRS. He obtained his PhD in numerical aerodynamics at Delft University of Technology in 2007. Since then, he has been responsible for the development of adaptive grid refinement in the Navier-Stokes solver ISIS-CFD.